Journal of Molecular Structure, 224 (1990) 7–20
Elsevier Science Publishers B.V., Amsterdam

VIBRATIONAL STUDIES OF THE DISULFIDE GROUP IN PROTEINS
Part II. Ab initio force fields and normal mode frequencies of dimethyl, methylethyl, and diethyl disulfides*,**

WENYUN ZHAO*** and SAMUEL KRIMM

Biophysics Research Division and Department of Physics, University of Michigan, Ann Arbor, MI 48109 (U.S.A.)

(Received 14 March 1989)

ABSTRACT

The geometric parameters and quadratic force constants of dimethyl disulfide, methylethyl disulfide, and diethyl disulfide in all their stable conformations and transition state conformations have been obtained from ab initio Hartree–Fock calculations with a 3-21G* basis set. Thirteen scale factors applied to the ab initio force field allow the reproduction of 62 observed frequencies with an average error of 0.5%. Relationships between the SS and CS stretch frequencies and the conformer internal rotation geometry are obtained. The results reported here provide a good basis for further investigation of the vibrational spectra of proteins containing cystine residues.

INTRODUCTION

Raman spectroscopy has been widely used to investigate the conformation of S–S bridges in proteins [1–6], since it is not difficult to obtain spectra in both solid and aqueous systems and the SS stretch, ν(SS), and CS stretch, ν(CS), modes are relatively stronger than other bands in the spectra. However, as reviewed in our previous paper [7], considerable controversy exists regarding the correlation of these frequencies with the internal rotation angles associated with the disulfide group.

We have initiated a vibrational spectroscopic study of this group by analyzing the spectra of alkyl disulfides through ab initio and normal mode calculations (see ref. 7, designated I, for the first paper in this series). Although several normal mode calculations have been done on dialkyl disulfides [8–10] and on a model of the S–S bridge in proteins [6], there are two major problems with these calculations. First, empirical force fields were used in which it was

*Dedicated to Professor Bryce L. Crawford, Jr.
**Part I is ref. 7.
***Permanent address: Institute of Theoretical Chemistry, Jilin University, Changchun, P.R. China.

0022-2860/90/$03.50

assumed that force constants are independent of the SS, τ(SS), and CS, τ(CS), dihedral angles. This contradicts results from CNDO/2 [11] and ab initio [12] calculations, which show that the SS bond length varies with τ(SS). Therefore, the correlation between vibrational frequencies and the internal torsion angles could not be obtained in reliable detail. Ab initio calculations, which are presented in this paper, provide the variation of force field with τ(SS) and τ(CS), and allow, with relatively few scale factors, the satisfactory reproduction of experimental frequencies. Based on such a scaled ab initio force field, normal mode calculations can thus provide a clear and reliable description of the correlation between the frequencies and torsion angles of the disulfide group. The second problem with the previous calculations is that they overlooked the difference between the structure in the real protein and that in the simple alkyl disulfides. We will treat this subject in later publications.

AB INITIO CALCULATIONS

The LCAO-MO-SCF restricted Hartree–Fock calculations were performed with the 3-21G* basis set, using the Gaussian 82 program for diethyl disulfide and methylethyl disulfide and the Gaussian 86 program for dimethyl disulfide. The geometries of conformers of $C_2H_5SSC_2H_5$ were obtained, at energy minima and maxima with respect to the nuclear coordinates, for τ(CS) corresponding to the *trans* (T) and *gauche* (G) (minima) and *cis* (C) and *skew* (S) (maxima) structures by simultaneous relaxation of all geometric parameters. (While we use these designations for angles near 180°, 60°, 0°, and 120°, respectively, we describe the minimum energy position of τ(SS), for convenience, as G even though its value is close to 90°.) Similarly, calculations were done for structures at the energy minima of $CH_3SSC_2H_5$ as a function of τ(CS) and for structures at both energy minima and maxima of CH_3SSCH_3 as a function τ(SS). In contrast to previous studies, the conformations with respect to the τ(CS) in $C_2H_5SSC_2H_5$ are more properly classified in terms of C, G, S, T, S′, and G′, where the prime means a rotation of τ(CS) opposite to that of τ(SS), because we believe that the relative stability, geometry, and characteristic vibrational frequencies should be different for G and G′, as well as for S and S′.

Some geometric parameters of $C_2H_5SSC_2H_5$ are listed in Table 1. Torsion angles together with relative energies of all conformers are listed in Table 2. These parameters will be used in normal mode calculations of protein model structures, which will be published later. (The geometry optimization for the transition state of the S′GG′ conformation did not converge with our procedure. Therefore τ(CS) had to be fixed at a constant value, −125.5°, which is the τ(CS) for the S′GS′ conformation, in optimizing all the other geometric parameters.) The relative energies of GXG conformations of $C_2H_5SSC_2H_5$ as

TABLE 1

Some geometric parameters of symmetric $C_2H_5SSC_2H_5$ conformers[a]

Parameter[b]	CGC	GGG	SGS	TGT	S′GS′	G′GG′
R(C-H)[c]	1.0848	1.0849	1.0848	1.0839	1.0848	1.0850
R(C-H)[d,e]	1.0809	1.0825	1.0829	1.0833	1.0831	1.0822
R(C-H)[e,f]	1.0815	1.0827	1.0809	1.0805	1.0806	1.0825
R(C-C)	1.535	1.536	1.539	1.541	1.539	1.533
R(C-S)	1.849	1.827	1.838	1.828	1.839	1.829
R(S-S)	2.035	2.045	2.042	2.044	2.043	2.056
θ(HCC)[e]	110.4	110.3	110.4	110.4	110.5	110.3
θ(CCS)	116.9	113.5	111.4	109.0	111.4	115.5
θ(HCS)[e]	105.7	106.8	107.8	109.0	107.8	106.0
θ(CSS)	107.7	103.1	104.4	102.9	104.4	103.7

[a]C, *cis*; G, *gauche*; S, *skew*; T, *trans*. [b]R in Å, θ in degrees. [c]Methyl group, H *trans* to S. [d]Methyl group, H *gauche* to S. [e]Average value. [f]Methylene group.

TABLE 2

Relative energies, torsion angles, and SS and CS stretch frequencies of $C_2H_5SSC_2H_5$ conformers[a]

Conformer	E (*kcal mol*$^{-1}$)	τ(CS) (deg)	τ(SS) (deg)	τ(SC) (deg)	ν(SS) (cm^{-1})	ν(CS) (cm^{-})	
GGG	0.00	69.4	86.3	69.4	504	638 (B)	646 (A)
GGT	0.20	69.4	86.6	177.6	525	642	669
TGT	0.40	177.6	86.6	177.6	542	667 (B)	670 (A)
GGG′	0.66	68.6	98.0	−69.1	499	638	646
TGG′	0.82	174.8	97.5	−68.6	523	640	669
GGS	1.80	68.2	87.2	119.9	513	639	649
GGS′	1.93	68.2	86.5	−123.9	511	641	649
SGT	1.98	120.0	87.4	177.1	532	646	668
SGG′	2.06	117.4	94.6	−69.5	508	639	648
TGS′	2.09	176.5	86.9	−123.8	531	648	669
G′GG′	2.36	−71.0	114.5	−71.0	497	635 (B)	642 (A)
S′GG′	2.42	−125.5	95.6	−74.4	507	639	649
SGS	3.69	118.7	89.8	118.7	520	641 (B)	650 (A)
SGS′	3.83	118.6	89.2	−125.5	518	644	650
CGG	3.93	−5.2	90.8	68.3	507	622	642
S′GS′	3.98	−125.5	88.6	−125.5	519	645 (B)	650 (A)
CGT	4.03	−4.7	90.8	174.0	527	625	668
CGG′	4.97	−12.6	105.7	−70.5	503	622	640
CGS	5.52	−1.8	89.3	116.5	513	623	646
CGS′	6.09	−6.7	97.3	−115.0	509	623	646
CGC	7.54	−11.6	95.7	−11.6	510	616 (B)	630 (A)

[a]C, *cis*; G, *gauche*; S, *skew*; T, *trans*.

a function of τ(SS) are given in Fig. 1. The 21 possible conformations of $C_2H_5SSC_2H_5$ are shown on a relative energy versus $R(C_1^{\alpha}-C_2^{\alpha})$ plot in Fig. 2, where $R(C_1^{\alpha}-C_2^{\alpha})$ is the distance between the two methyl carbon atoms, which would correspond to the C^{α}–C^{α} distance in the cystine bridge of proteins. Most disulfides prefer the lowest energy conformations, GGG and GGT. However if strain exists, for example in a crystal or a protein molecule, conformations with relatively higher energies can occur, and in small ring structures G′GG′ and S′GG′ are possible. Almost all of the 21 disulfide conformations are found in proteins. In a survey of the crystal structures of 15 proteins [6], encompassing

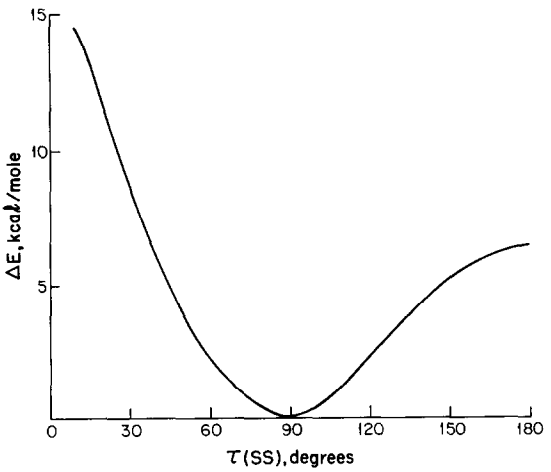

Fig. 1. Relative energy of GXG conformers of $C_2H_5SSC_2H_5$ as a function of τ(SS), the SS dihedral angle (the energy of GGG is taken as zero).

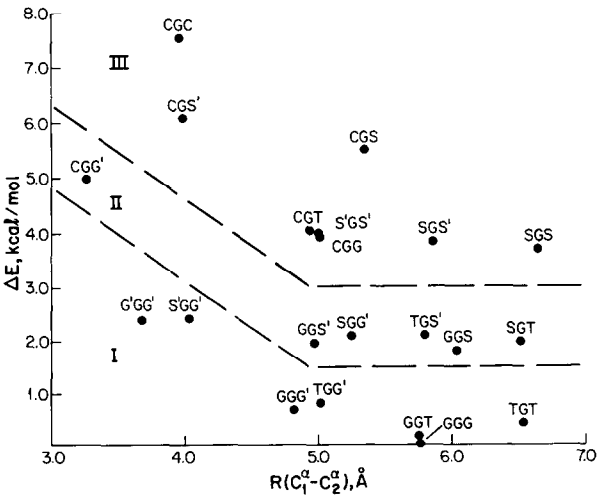

Fig. 2. Relative energy of $C_2H_5SSC_2H_5$ conformers as a function of $R(C_1^{\alpha}-C_2^{\alpha})$, the $(H_3)C$-$C(H_3)$ distance (see text for definitions of regions I, II, and III).

61 disulfide bridges, 42 conformers (69%) fell into the group of 7 designated as class I in Fig. 2, 12 (20%) into the 6 of class II, and 8 (11%) into the remaining 8 of class III. (The G′GG′ and S′GG′ conformers are included in class I even though they have a higher energy because they are relatively numerous and represent the lowest energy strained, viz., small $R(C_1^{\alpha}-C_2^{\alpha})$, structures.)

The force fields in cartesian coordinates for the disulfide molecules were calculated using the ab initio Gaussian 82 and Gaussian 86 (only for CH_3SSCH_3) programs. Only the Gaussian 86 program calculated Raman and IR intensities, and because at this time we could not use it to calculate molecules larger than CH_3SSCH_3, such intensities were not obtained for $CH_3SSC_2H_5$ and $C_2H_5SSC_2H_5$. The calculations were carried out on an IBM-3090, except that the force fields of $CH_3SSC_2H_5$ and $C_2H_5SSC_2H_5$ were carried out on a Micro VAX II. Because of the extensive computations, the force field calculations for $C_2H_5SSC_2H_5$ were carried out only for the six symmetric conformers, CGC, GGG, SGS, TGT, S′GS′, G′GG′, and one asymmetric conformer GGT, which is the second most stable conformer and for which some experimental frequencies are known.

NORMAL MODE CALCULATIONS

A total of 26, 36, and 46 internal coordinates were defined for dimethyl, methylethyl, and diethyl disulfides, respectively, in the traditional way [13], 2, 3, and 4 of these, respectively, being redundant coordinates. The **B** matrices of these molecules in their various conformations were calculated in the standard manner. The $\mathbf{F}_x$ matrices in cartesian coordinates from the ab initio calculations were transformed into **F** matrices in internal coordinates in the following way. By diagonalizing the product matrix $\mathbf{B}\tilde{\mathbf{B}}$ (where $\sim$ indicates the transpose) with a unitary matrix **U**, the eigenvalue matrix $\mathbf{\Gamma}$ is obtained

$$\tilde{\mathbf{U}}(\mathbf{B}\tilde{\mathbf{B}})\mathbf{U}=\mathbf{\Gamma}$$

The non-zero eigenvalue matrix, $\mathbf{\Gamma}_0$, and corresponding eigenvectors $\mathbf{U}_0$

$$\mathbf{U}=(\mathbf{U}_0\mathbf{U}_1) \qquad \mathbf{\Gamma}=\begin{pmatrix}\mathbf{\Gamma}_0 & 0\\ 0 & 0\end{pmatrix}$$

are used to calculate the generalized inverse matrix of **B** by

$$\mathbf{B}^{\dagger}=\tilde{\mathbf{B}}\mathbf{U}_0\mathbf{\Gamma}_0^{-1}\tilde{\mathbf{U}}_0$$

The force constants are then transformed from cartesian coordinates to internal coordinates by

$$\mathbf{F}=\tilde{\mathbf{B}}^{\dagger}\mathbf{F}_x\mathbf{B}^{\dagger}$$

Since ab initio force constants generally give vibrational frequencies that are considerably higher than experimental values, the force constants must be

scaled. The scaling procedure used was as follows. The internal coordinates were separated into different groups according to their chemical types, for example, CH stretch, CCH bend, HCH bend, etc., and a scale factor C_i was assigned to group i. Then the diagonal force constant F_{ii} was multiplied by C_i and the off-diagonal force constant F_{ij} by $(C_iC_j)^{1/2}$, or in matrix notation [14]

$$\mathbf{F} = C^{1/2}\mathbf{F}^{ab}C^{1/2}$$

where $\mathbf{F}^{ab}$ is the $\mathbf{F}$ matrix in internal coordinates from the ab initio calculation. The $\mathbf{F}^{ab}$ matrix obtained by the above procedure is a canonic $\mathbf{F}$ matrix [15]. To keep the $\mathbf{F}$ matrix after scaling canonic, the following transformation was performed.

$$\mathbf{F}_c = \mathbf{U}_0\tilde{\mathbf{U}}_0\mathbf{F}\mathbf{U}_0\tilde{\mathbf{U}}_0$$

To check the $\mathbf{B}$ and $\mathbf{F}$ matrices obtained for each conformation, all scaling factors were initially kept fixed at a value of 1.0 in order to reproduce the pure ab initio calculated vibrational frequencies. Subsequently, scaling factors of 0.9 for stretching and torsional coordinates and 0.8 for bending coordinates were used to get vibrational frequencies, eigenvectors, and potential energy distributions (PED) in the symmetry coordinates. The vibrational spectra were assigned by comparing the initial calculations with experimental data [16–19]. The assignments were generally the same as in previous studies [8, 9], except for some small modifications. The experimental frequencies used in the assignments and in the optimization of scale factors were modified slightly by our Raman results. Subsequently, the scale factors were optimized to give the best fit to the observed frequencies. The final scale factors are listed in Table 3. These scale factors also apply to the selected ab initio force constant set, to be published in our next paper [20], which is the basis for normal mode calculations on more complex molecules. The observed frequencies for low energy

TABLE 3

Scale factors for force constants of CH_3SSCH_3, $CH_3SSC_2H_5$ and $C_2H_5SSC_2H_5$

Coordinate[a]	Scale factor	Coordinate[a]	Scale factor
SS s	0.870	CCS b	0.820
SC(H_3)[b] s	0.875	SCH b	0.740
SC(CH_3)[c] s	0.862	CCH b	0.792
CC s	0.920	HCH b	0.748
CH s	0.820	SS tor	1.130
CSS b	0.875	CS[d] tor	1.000
		CH_3 tor	0.820

[a]s, Stretch; b, bend; tor, torsion. [b]Methyl carbon. [c]Methylene carbon. [d]Fixed value.

conformers, with associated calculated values using the full ab initio force field, are listed in Tables 4–6.

It can be seen from these results that the ab initio force field allows for a more detailed description than do the empirical force fields [8, 9]. For example, the best of these previous calculations [9] gave almost the same frequencies (2 cm^{-1} difference) for the four ν(CS) frequencies of the GGG and GGT conformers of $C_2H_5SSC_2H_5$. This is not consistent with the experimental data, which show that the ν(CS) frequency of the GGT conformer is about 27 cm^{-1} higher than that of the GGG conformer, in good agreement with our calculations. Moreover, in our Raman polarization experiments [20], when the electric vector of the scattered beam is rotated from the parallel to the perpendic-

TABLE 4

Observed and calculated frequencies and intensities of CH_3SSCH_3

Observed[a]		Calculated					
Raman	IR	Freq	Sym	I(R)	I(IR)	PED[b]	
2990 m	2986 s	2997	A	111	5.2	CH_3 as(100)	
		2997	B	0	8.1	CH_3 as(100)	
2983 m		2980	A	149	7.4	CH_3 as(99)	
		2978	B	11	3.3	CH_3 as(99)	
2913 s	2915 vs	2912	A	227	19.1	CH_3 ss(98)	
		2910	B	2	19.6	CH_3 ss(98)	
1426 m	1430 vs	1430	B	25	22.7	CH_3 ab(96)	
		1426	A	7	0.8	CH_3 ab(96)	
1419 m	1415 vs	1422	A	41	10.5	CH_3 ab(95)	
		1417	B	11	15.9	CH_3 ab(96)	
1311 mw		1323	A	3	0.2	CH_3 sb(107)	
	1303 vs	1317	B	2	1.1	CH_3 sb(109)	
	955 vs	958	B	5	22.0	CH_3 r(84)	CH_3 r(94)
949 m		952	A	9	7.3	CH_3 r(85)	CH_3 r(95)
		945	A	11	2.7		
		937	B	0	3.4		
694 vs	691 m	694	A	26	0.9	CS s(104)	
691 m		688	B	21	1.1	CS s(107)	
509 vs	511 mw	508	A	27	0.3	SS s(100)	
274 ms	276 m	274	B	3	1.2	CSS b(97)	CH_3 r(14)
240 s	241 m	240	A	4	1.5	CSS b(88)	CH_3 r(10)
		157	B	0	0.5	CS tor(96)	
		150	A	1	0.1	CS tor(91)	CSS b(19)
114 ms		114	A	2	1.5	SS tor(93)	

[a]Ref. 16; in cm^{-1}. [b]Potential energy distribution, components $\geq 10\%$; a = antisymmetric, s = symmetric; s = stretch, b = bend, r = rock; tor = torsion.

TABLE 5

Observed and calculated frequencies of $CH_3SSC_2H_5$

Obs.[a]	GG Conformer		GT Conformer	
	Calc.	PED[b]	Calc.	PED[b]
	2997	(S)CH_3 as(100)	2997	(S)CH_3 as(100)
	2980	(C)CH_3 as(58) CH_2 as(29) (S)CH_3 as(12)	2989	CH_2 as(82) (C)CH_3 as(16)
	2979	(S)CH_3 as(86)	2979	(S)CH_3 as(99)
2962*	2960	(C)CH_3 as(58) CH_2 as(34)	2962	(C)CH_3 as(90)
	2954	(C)CH_3 as(70) CH_2 as(29)	2958	(C)CH_3 as(89) CH_2 as(12)
	2919	CH_2 ss(90)	2935	CH_2 ss(92)
2907*	2910	(S)CH_3 ss(98)	2911	(S)CH_3 ss(98)
	2901	(C)CH_3 ss(93)	2903	(C)CH_3 ss(100)
1453*	1452	(C)CH_3 ab(91)	1449	(C)CH_3 ab(91)
1437*	1444	(C)CH_3 ab(90)	1446	(C)CH_3 ab(90) (C)CH_3 r(10)
	1428	(S)CH_3 ab(94)	1431	CH_2 b(71) (S)CH_3 ab(26)
1418*	1420	(S)CH_3 ab(70) CH_2 b(26)	1427	(S)CH_3 ab(69) CH_2 b(29)
	1415	CH_2 b(71) (S)CH_3 ab(27)	1419	(S)CH_3 ab(95)
1380*	1382	(C)CH_3 sb(105)	1382	(C)CH_3 sb(106)
1307*	1320	(S)CH_3 sb(107)	1320	(S)CH_3 sb(107)
1282*	1266	CH_2 w(85)	1264	CH_2 w(91)
1255*	1250	CH_2 tw(53) (C)CH_3 r(19)	1242	CH_2 tw(52) (C)CH_3 r(22)
1050*	1051	(C)CH_3 r(53) CC s(30) CH_2 w(13)	1050	(C)CH_3 r(58) CC s(19) CH_2 w(11)
1030*	1031	CH_2 tw(41) (C)CH_3 r(40) CH_2 r(17)	1019	CH_2 tw(48) (C)CH_3 r(37) CH_2 r(19)
969*	967	CC s(66) (C)CH_3 r(19)	966	CC s(77) (C)CH_3 r(11)
954*	955	(S)CH_3 r(83)	955	(S)CH_2 r(83)
	941	(S)CH_3 r(94)	941	(S)CH_3 r(93)
781			774	CH_2 r(73) (C)CH_3 r(35)
759	757	CH_2 r(74) (C)CH_3 r(32)		
692	692	(H_3)CS s(105)	692	(H_3)CS s(105)
669			668	(H_2)CS s(91) (C)CH_3 r(10)
641	641	(H_2)CS s(94) SCC b(11)		
524			528	SS s(93)
509	506	SS s(99)		
362	361	SCC b(68) SSC(H_2) b(18)		
327			329	SCC b(37) SSC(H_2) b(13) (H_3)CSS b(12)
280	286	(H_3)CSS b(41) SSC(H_2) b(23) (H_3)CC tor(29)		
246			248	(H_3)CSS b(82) (S)CH_3 r(10)
	236	(H_3)CSS b(49) (H_3)CC tor(47)		
			226	(H_3)CC tor(82)
196	195	(H_2)CSS b(46) (H_3)CC tor(16) SCC b(14) (H_3)CS tor(14)	193	(H_2)CSS b(51) SCC b(29) (H_3)CS tor(23)
	150	(H_3)CS tor(85) (H_2)CSS b(19)	143	(H_3)CS tor(77) (H_2)CSS b(30)
	118	SS tor(46) (H_2)CS tor(45)	106	SS tor(87)
	75	(H_2)CS tor(58) SS tor(49)	66	(H_2)CS tor(97)

[a]Refs. 17 and 18; in cm^{-1}. Values marked with an asterisk are from infrared spectrum; others from Raman spectrum. [b]Potential energy distribution, components ≥10%: a = antisymmetric, s = symmetric; s = stretch, b = bend, w = wag, tw = twist, r = rock, tor = torsion.

TABLE 6

Observed and calculated frequencies of $C_2H_5SSC_2H_5$

Obs.[a]	GGG Conformer		GGT Conformer	
	Calc.	PED[b]	Calc.	PED[b]
	2980 *A*	CH_3 as(66) CH_2 as(33)	2988	CH_2 as(83) CH_3 as(16)
	2980 *B*	CH_3 as(70) CH_2 as(29)	2980	CH_3 as(66) CH_2 as(33)
2959	2961 *A*	CH_3 as(55) CH_2 as(35)	2961	CH_3 as(89)
	2960 *B*	CH_3 as(59) CH_2 as(33)	2960	CH_3 as(57) CH_2 as(35)
	2954 *A*	CH_3 as(73) CH_2 as(26)	2958	CH_3 as(87) CH_2 as(13)
	2954 *B*	CH_3 as(65) CH_2 as(33)	2954	CH_3 as(73) CH_2 as(26)
2915	2919 *A*	CH_2 ss(89)	2935	CH_2 ss(92)
	2918 *B*	CH_2 ss(91)	2918	CH_2 ss(90)
	2901 *A*	CH_3 ss(93)	2903	CH_3 ss(100)
	2900 *B*	CH_3 ss(93)	2900	CH_3 ss(93)
1446	1452 *B*	CH_3 ab(91)	1449	CH_3 ab(91)
	1452 *A*	CH_3 ab(91)	1452	CH_3 ab(91)
	1444 *A*	CH_3 ab(90)	1444	CH_3 ab(90)
	1444 *B*	CH_3 ab(90)	1446	CH_3 ab(90)
1418	1417*A*	CH_2 b(98)	1430	CH_2 b(100)
	1416 *B*	CH_2 b(99)	1416	CH_2 b(99)
1374*	1383 *B*	CH_3 sb(105)	1382	CH_3 sb(105)
	1382 *A*	CH_3 sb(105)	1382	CH_3 sb(105)
1278*	1272 *A*	CH_2 w(83)	1270	CH_2 w(84)
1254	1260 *B*	CH_2 w(88)	1260	CH_2 w(91)
	1251 *A*	CH_2 tw(51) CH_3 r(19)	1241	CH_2 tw(52) CH_3 r(22)
	1250 *B*	CH_2 tw(55) CH_3 r(19)	1251	CH_2 tw(52) CH_3 r(19)
1050	1053 *A*	CH_3 r(53) CC s(29) CH_2 w(12)	1051	CH_3 r(54) CC s(27) CH_2 w(12)
	1048 *B*	CH_3 r(52) CC s(30) CH_2 w(13)	1049	CH_3 r(59) CC s(22) CH_2 w(11)
1029	1033 *B*	CH_2 tw(41) CH_3 r(40) CH_2 r(17)	1031	CH_2 tw(41) CH_3 r(41) CH_2 r(17)
	1028 *A*	CH_2 tw(41) CH_3 r(40) CH_2 r(17)	1019	CH_2 tw(48) CH_3 r(37) CH_2 r(19)
967	967 *A*	CC s(66) CH_3 r(20)	967	CC s(69) CH_3 r(19)
	967 *B*	CC s(67) CH_3 r(20)	966	CC s(77) CH_3 r(13)
781*			774	CH_2 r(73) CH_3 r(35)
760	758 *B*	CH_2 r(74) CH_3 r(32)	757	CH_2 r(74) CH_3 r(32)
	755 *A*	CH_2 r(75) CH_3 r(31)		
668			669	CS s(92) CH_3 r(10)
643	646 *A*	CS s(92) CCS b(11)		
640*	638 *B*	CS s(98) CCS b(11)	642	CS s(94) CCS b(11)
523			525	SS s(91)
508	504 *A*	SS s(97)		

TABLE 6 (continued)

Obs.[a]	GGG Conformer		GGT Conformer	
	Calc.	PED[b]	Calc.	PED[b]
366	370 *A*	CCS b(66) SSC b(20)	361	CCS b(66) SSC b(21)
357	351 *B*	CCS b(65) SSC b(20)		
328			331	CCS b(39) SSC b(20)
287	285 *B*	SSC b(40) (H_3)CC tor(40) CCS b(23)		
255	253 *A*	(H_3)CS tor(84)	260	(H_3)CS tor(58) CCS b(18) SSC b(16)
			226	(H_3)CC tor(90)
200	206 *B*	(H_3)CC tor(53) SSC b(39)	199	SSC b(52) (H_2)CC tor(30) CCS b(20)
180	172 *A*	SSC b(76) CCS b(17)	175	SSC b(75) CCS b(26)
	124 *A*	CS tor(75) SS tor(23)	107	CS tor(43) SS tor(39)
	82 *B*	CS tor(96)	79	CS tor(80) SS tor(31)
	58 *A*	SS tor(73) CS tor(34)	56	CS tor(75) SS tor(20)

[a]Refs. 17 and 19; in cm^{-1}. Values marked with an asterisk are from infrared spectrum; others from Raman spectrum. [b]Potential energy distribution, components $\geq 10\%$: a = antisymmetric, s = symmetric; s = stretch, b = bend, w = wag, tw = twist, r = rock, tor = torsion.

ular orientation, the ν(CS) frequency of $C_2H_5SSC_2H_5$ at 643 cm^{-1} shifts down 3 cm^{-1}. Because of limitations on experimental resolution and the overlapping of three ν(CS) modes, it is expected that the real difference between the frequencies of the symmetric and antisymmetric stretching modes is probably more than 3 cm^{-1}, which is consistent with our calculation which gives the difference of these two frequencies as 8 cm^{-1}. We found a similar frequency red-shift, 3.5 cm^{-1}, in the spectrum of CH_3SSCH_3, although only a 1 cm^{-1} red-shift was reported previously [16].

The present assignments of ν(CS) modes of $C_2H_5SSC_2H_5$ (643 and 640 cm^{-1}) and CH_3SSCH_3 (694 and 691 cm^{-1}) are based on our Raman polarization experiments, which indicate that the symmetric ν(CS) mode is higher than the antisymmetric mode. The symmetric CCH_3 torsion frequency of GGG $C_2H_5SSC_2H_5$ is predicted at 253 cm^{-1} and the corresponding frequency of the GGT conformer is at 260 cm^{-1} by our calculations. Therefore we assign the Raman band at 255 cm^{-1} to the overlap of these modes (Table 6), whereas Sugeta [9] assigns the 255 cm^{-1} band to the CCH_3 torsion of only the GGT conformer. The CH_2 twist mode by a previous calculation [9] is much purer (92%) than by our calculation; unfortunately, it is difficult at present to determine the approximate PED values from experimental data. For $CH_3SSC_2H_5$, our assignments are very similar to Sugeta's [9] except in the PED values for the CH_2 twist mode. Additionally, the SSC bend frequency of the GT con-

former, 248 cm^{-1}, is by our calculation 12 cm^{-1} lower than Sugeta's value [9] and is thus closer to the experimental value. The only difference in the assignments for CH_3SSCH_3 is in the CH_3 rock vibration. The calculation of Sugeta et al. [2] gives the symmetric CH_3 rock a higher frequency, 950 cm^{-1}, than the corresponding antisymmetric mode, 948 cm^{-1}, whereas our calculation predicts the opposite, 958 (B) and 952 (A) cm^{-1}, which is consistent with the observed and calculated Raman and IR intensities (see Table 4).

FORCE CONSTANTS AND VIBRATIONAL FREQUENCIES AS A FUNCTION OF CS TORSION ANGLE

The variation of the SS stretch force constant, $f(SS)$, and the SS stretch frequency with $\tau(SS)$ in CH_3SSCH_3 were shown in Fig. 1 of our previous paper [7]. A similar variation was found in $C_2H_2SSC_2H_5$ from our present calculations. We have therefore assumed that $f(SS)$ in $C_2H_5SSC_2H_5$ varies in the same way as in CH_3SSCH_3. Since we found that the $\nu(SS)$ and $\nu(CS)$ frequencies are more dependent on $\tau(CS)$ than on $\tau(SS)$, we have studied the correlation with $\tau(CS)$ in more detail. (The variation of $f(SS)$ and $\nu(SS)$ with $\tau(SS)$ in CH_3SSCH_3 is quite small near the optimum conformation [7]: $f(SS)$ decreases by ~ 0.03 mdyn $Å^{-1}$ for a $\pm 15°$ change from $\tau(SS) = 84°$, and $\nu(SS)$ decreases by ~ 1.5 cm^{-1} for a $\pm 15°$ change from $\tau(SS) = 93°$. In our next paper [20], we will show how to make corrections to the following results for small changes in $\tau(SS)$.)

Normal mode calculations were done for all 21 possible conformers of $C_2H_5SSC_2H_5$ using the full scaled ab initio force field described above. All of the geometric parameters for the asymmetric conformers were taken directly from the ab initio calculations (see Table 1), while the **F** matrices had to be determined by approximation. Our method is illustrated by the CGG conformer. In this case, all the force constants for the *cis* side were taken from the values for the CGC conformer, and for the *gauche* side from the GGG conformer. The diagonal SS stretch and SS torsion force constants and all the off-diagonal constants belonging to both sides were taken as the average value from both CGC and GGG conformers. The off-diagonal elements of SS stretch and SS torsion received 3/4 of their value from the symmetric conformation corresponding to the side of the molecule in which the internal coordinate other than SS stretch or SS torsion was located and 1/4 from the other symmetric conformation. The frequencies calculated using this algorithm for the GGT conformer were very close to those obtained directly from the scaled ab initio force field, with at most 1 or 2 cm^{-1} difference.

The $\nu(SS)$ and $\nu(CS)$ frequencies of the symmetric conformer of $C_2H_5SSC_2H_5$ are plotted as a function of $\tau(CS)$ in Fig. 3 and the $\nu(SS)$ and $\nu(CS)$ frequencies for all 21 conformations are listed in Table 2. Because the $\nu(CS)$ frequency splits for the symmetric $C_2H_5SSC_2H_5$, the average value of

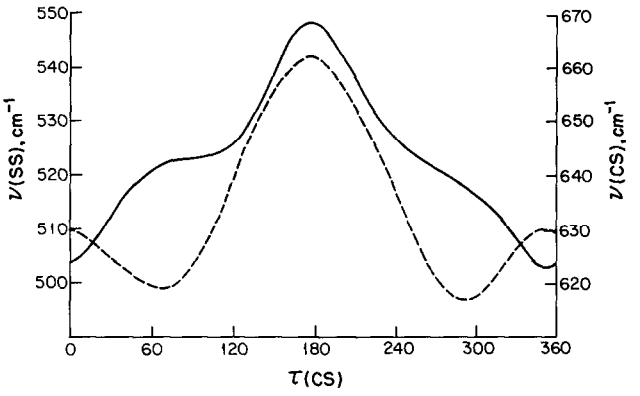

Fig. 3. Dependence of ν(CS), the CS stretch frequency (—), and ν(SS), the SS stretch frequency (---), on τ(CS), the CS dihedral angle, for XGX $C_2H_5SSC_2H_5$.

the symmetric and antisymmetric ν(CS) frequencies is used in Fig. 3. It is interesting that the ν(SS) frequency has two maxima, at the *trans* and *cis* conformations, whereas the ν(CS) frequency has only one. From the ab initio calculations, we know that the SS and CS force constants vary by about 4% as τ(CS) changes; therefore the variation of the force constants themselves probably gives rise to only about a 2% variation in the frequencies. Since these frequencies vary by about 7% as τ(CS) changes (cf. Fig. 3), we conclude that the geometric factor is more responsible for the variation in ν(SS) and ν(CS) frequencies than are the force constants. However, keeping the force constants fixed will also cause considerable error if a more detailed description of the normal modes is needed. The ν(SS) frequencies follow the order: TT > SS > S′S′ > CC > GG > G′G′ whereas the ν(CS) frequencies follow a slightly different order: TT > S′S′ > SS > GG > G′G′ > CC.

Our results show for the first time that the frequencies of the G and G′ conformers are not the same, the ν(SS) of these two conformers differing by 7 cm^{-1}. The frequencies of the S and S′ conformers are also different, although the difference is much smaller. Another important conclusion from our calculations is that the ν(CS) frequency depends mainly on the geometry of one side of the SS bridge, the effect of τ(CS) of the other side of the SS bridge being very small. However, the ν(SS) frequency depends on the τ(CS) angles on both sides. This dependence has already been shown by Sugeta et al. [2] based on experimental data.

According to our calculations, the ν(SS) frequency of the GGG conformer of $C_2H_5SSC_2H_5$ is 21 cm^{-1} lower than that of the GGT conformer, whereas the observed difference is 15 cm^{-1}. It seems that our calculations overstate the difference between different conformers. Although we tried to avoid this difficulty by reducing the scale factor for the interaction force constants between SS stretch and other coordinates, it could not be eliminated. Based on this

argument, the ν(SS) frequency of the TGT conformer may not be as high as given by our calculation, viz., 542 cm^{-1}. We attempted to observe the ν(SS) band of the TGT conformer by increasing the temperature of the $C_2H_5SSC_2H_5$ sample, but no clear effect was seen. This is puzzling in view of the calculated energy difference of only 0.4 kcal mol^{-1} between the TGT and GGG conformers.

CONCLUSIONS

The use of 13 refined scale factors to the ab initio force constants of CH_3SSCH_3, $CH_3SSC_2H_5$ and $C_2H_5SSC_2H_5$ has permitted the reproduction of 62 observed IR and Raman frequencies with an average error of 0.5%. These results enable us to use a selected set of these force constants [20] to calculate the normal modes of more complex disulfide molecules. We have also been able to show how the SS and CS stretch frequencies depend on the internal rotation geometry of the disulfide group. Such studies should permit a more detailed characterization of the cystine bridge geometry in proteins by Raman spectroscopy than has heretofore been possible.

ACKNOWLEDGEMENT

We are indebted to Dr. J. Bandekar for the Raman polarization studies. This research was supported by a grant from the Monsanto Company, St. Louis, MO.

REFERENCES

1 R.C. Lord and Nai-teng Yu, J. Mol. Biol., 50 (1970) 509.
2 H. Sugeta, A. Go and T. Miyazawa, Chem. Lett., 83 (1972).
3 H. Brunner and M. Holz, Biochim. Biophys. Acta, 379 (1975) 408.
4 H.E. Van Wart and H.A. Scheraga, J. Phys. Chem., 80 (1976) 1812, 1823.
5 T. Takamatsu, I. Harada and K. Hayashi, Biochim. Biophys. Acta, 622 (1980) 189.
6 A.H. Kuptsov and V.I. Trofimov, J. Biomol. Struct. Dyn., 3 (1985) 185.
7 W. Zhao, J. Bandekar and S. Krimm, J. Am. Chem. Soc., 110 (1988) 6891, and references cited therein.
8 D.W. Scott and M.Z. El-Sabban, J. Mol. Spectrosc., 31 (1969) 362.
9 H. Sugeta, Spectrochim. Acta, Part A, 31 (1975) 1729.
10 B.E. Weiss-Lopez, M.H. Goodrow, W.K. Musker and C.P. Nash, J. Am. Chem. Soc., 108 (1986) 1271.
11 H.E. Van Wart, L.L. Shipman and H.A. Scheraga, J. Phys. Chem., 78 (1974) 1848.
12 M. Aida and C. Nagata, Theor. Chim. Acta, 70 (1986) 73.
13 E.B. Wilson, Jr., J.C. Decius and P.C. Cross, Molecular Vibrations, McGraw-Hill, New York, 1955.
14 G. Fogarasi and P. Pulay, in J.R. Durig (Ed.), Vibrational Spectra and Structure, Vol. 4, Elsevier, Amsterdam, 1985.
15 K. Kuczera and R. Czerminksi, J. Mol. Struct., 105 (1983) 269.

16 S.G. Frankiss, J. Mol. Struct., 3 (1969) 89.
17 H. Sugeta, A. Go and T. Miyazawa, Bull. Chem. Soc. Jpn., 46 (1973) 3407.
18 K.G. Allum, J.A. Creighton, J.H. Green, G.J. Minkoff and L.J.S. Prince, Spectrochim. Acta, Part A, 24 (1968) 927.
19 D.W. Scott, H.L. Finke, J.P. McCullough, M.E. Gross, R.E. Pennington and G. Waddington, J. Am. Chem. Soc., 74 (1952) 2478.
20 W. Zhao, J. Bandekar, and S. Krimm, J. Mol. Struc., in press.